Determination of the Spin Distribution in Nitronylnitroxides by Solid-State ^{1}H, ^{2}H, and ^{13}C NMR Spectroscopy

Henrike Heise,[1a] Frank H. Köhler,*,[1a] Fernando Mota,[1b] Juan J. Novoa,[1b] and Jaume Veciana[1c]
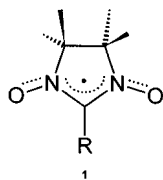
Contribution from the Anorganisch-chemisches Institut, Technische Universität München D-85747 Garching, Germany, Departament de Química Física, Facultat de Química, Universitat de Barcelona, Av. Diagonal 647, E-08028 Barcelona, Spain, and Institut de Ciència de Materials de Barcelona (CSIC), Campus Universitari de Bellaterra, E-08913 Cerdanyola, Spain

Abstract: Nitronylnitroxide radicals substituted by 2′-hydroxy-, 3′-hydroxy-, 4′-hydroxy-, and 4′-methoxyphenyl groups and by a methyl group (**2**, **3**, **4**, **5**, and **6**, respectively) have been investigated in the solid state with ^{1}H, ^{2}H, and ^{13}C NMR spectroscopy under magic angle spinning (MAS) and in solution with ^{1}H and ^{2}H NMR spectroscopy. Well-resolved ^{13}C MAS NMR spectra have been recorded which show signals in ranges up to almost 1900 ppm. The ^{1}H NMR signal spread does not exceed 60 ppm (except for a unique methyl signal of **6** near −230 ppm), and the resolution is worse than that of ^{13}C NMR spectra. Narrower signals have been obtained with ^{2}H NMR spectroscopy. The signals have been assigned with the help of various criteria including the results of ab initio calculations. From the NMR data it has been concluded that the nitronylnitroxide five-ring is puckered, thus rendering all substituents inequivalent. Signal coalescence at elevated temperatures has shown that these inequivalencies are partly averaged out while the puckering is maintained. Dynamics of this sort have not been observed when OH···ON bridges render the lattice more rigid. The spin densities at the carbon and hydrogen atoms have been obtained from the NMR data. They are in accord with theoretical results in the limit of approximation. The spin maps so obtained confirm that the polarization mechanism determines the spin distribution in **2**−**6**. The distribution is modulated by hyperconjugation and competing polarization paths. It is concluded that solid-state NMR spectroscopy may be an alternative to polarized neutron diffraction in evaluating the spin distribution in radicals. The weak and strong points of the method are discussed.

Introduction

When nitronylnitroxides of the general formula **1**[2] were first synthesized 31 years ago,[3] chemists were mainly attracted by the fact that these radicals exhibit a remarkable thermal and redox stability. This chemistry has experienced a renaissance since the advent of transition-metal derivatives[4] which feature new properties such as ferro-, ferri-, and antiferromagnetism. Of particular interest is spontaneous magnetization known for some examples since 1989,[5] because this has established "the metal-radical approach toward molecular magnets".[4a]

1

In 1991 ferromagnetic ordering of a metal-free nitronylnitroxide has been published.[6] This has triggered a boom of recently reviewed[7] work, so that there is now also a "pure nitronylnitroxide approach toward molecular magnets". For the systematic assembly of nitronylnitroxide magnets one would expect two features to play a key role: the crystal architecture and the distribution of the unpaired spin in the molecule. Thus, the radicals should be arranged in the crystal in such a way that the sum of the interactions between various centers of neighboring species is ferromagnetic. The interplay of these interactions must be complex, because no magneto-structural correlation could be established in a recent survey.[8]

The spin densities come into play when individual inter-radical contacts are considered.[9] Conceptually, the unpaired electron is first delocalized in the molecule and/or spin is induced at various atoms. Then through-space exchange interaction between the spin densities ρ_i^A and ρ_j^B (at nuclei i and j of radicals A and B, respectively) is allowed. To achieve ferromagnetic interaction according to the McConnell-I[9,10] model

(1) (a) Technische Universität München. (b) Universitat de Barcelona (c) CSIC.

(2) While the rational name 2-*R*-4,4,5,5-tetramethyl-4,5-dihydro-1*H*-imidazol-1-oxy-3-oxide describes one limiting structure, **1** emphasizes the fact that the radicals have C_{2v} symmetry (for simple *R*) in solution with slight deviation of the spin distribution from C_{2v} in the solid state.

(3) Osiecki, J. H.; Ullman, E. F. *J. Am. Chem. Soc.* **1968**, *90*, 1078−1079.

(4) (a) Caneschi, A.; Gatteschi, D.; Sessoli, R. *Acc. Chem. Res.* **1989**, *22*, 392−398. (b) Caneschi, A.; Gatteschi, D.; Rey, P. *Prog. Inorg. Chem.* **1991**, *39*, 331−429.

(5) Caneschi, A.; Gatteschi, D.; Renard, J. P.; Rey P.; Sessoli R. *Inorg. Chem.* **1989**, *28*, 1976−1980.

(6) Turek, P.; Nozawa, K.; Shiomi, D.; Awaga, K.; Inabe, T.; Maruyama, Y.; Kinoshita, M. *Chem. Phys. Lett.* **1991**, *180*, 327−331.

(7) (a) Veciana, J.; Cirujeda, J.; Rovira, C.; Vidal-Gancedo, *J. Adv. Mater.* **1995**, *7*, 221−225. (b) Kinoshita, M. *Handbook of Organic Conductive Molecules and Polymers*; Nalwa, H. S., Ed.; Wiley: Chichester, New York, Weinheim, Brisbane, Singapore, Toronto 1997; Vol. 1, Chapter 15. (c) Nakatsuji, S.; Anzai, H. *J. Mater. Chem.* **1997**, *7*, 2161−2174.

(8) Deumal, M.; Cirujeda, J.; Veciana, J.; Novoa, J. J. *Chem. Eur. J.* **1999**, *5*, 1631−1642.

(9) (a) Kollmar, C.; Kahn, O. *Acc. Chem. Res.* **1993**, *26*, 259−265. (b) Okumura, M.; Mori, W.; Yamaguchi, K. *Mol. Cryst. Liq. Cryst.* **1993**, *232*, 35−44.

the spin density product $\rho_i^A \rho_j^B$ must be negative. This model has been extended,[11] and it has been shown to work although it is not rigorously valid.[12] Even so, it is generally important to know the sign and the amount of the spin density at each radical site to theoretically describe the magnetism.
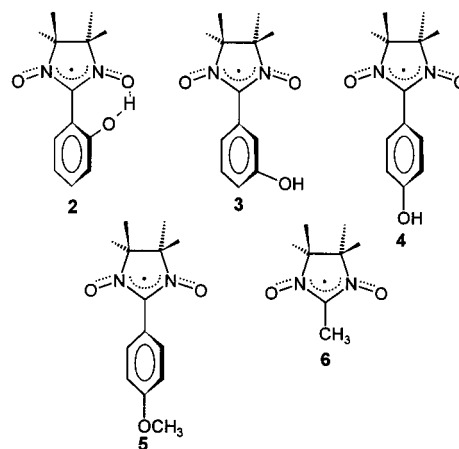
Up to now electron resonance methods are most popular for the determination of spin densities. For instance, ESR spectroscopy has shown that in nitronylnitroxides much spin density is located at the two nitrogen atoms.[3,13] High-resolution ESR yields additional information on most of the hydrogen atoms,[13] and this has been particularly useful for the hydroxyphenyl derivatives of the present study.[14] However, the sign of the spin density could not be determined experimentally by ESR. ENDOR spectroscopy is another high-resolution method which has been applied to nitronylnitroxides.[15] In theses studies spin signs have been obtained by working in the triple resonance mode. However, the latter studies are not routine so that the general limitations of electron resonance are: (i) Data of pure crystalline radicals are not available, (ii) it is difficult to determine the spin sign, and (iii) carbon nuclei are not accessible except for a unique site.[13b] This is unfortunate, because points (i)−(iii) are important for the understanding of magnetic interactions.

Polarized neutron diffraction (PND) is the most powerful method for the determination of spin densities known so far. It has been applied to nitronylnitroxides,[16] and in landmark studies rather complete spin maps including the signs have been obtained for the phenyl[16a] and the 4-nitrophenyl derivatives.[16b] It is noteworthy that PND also detects the spin on oxygen which has not been determined by any other method mentioned here.

Pioneering NMR work on nitronylnitroxides in solution has furnished the first data for hydrogens and carbons that include the spin sign.[13a,17] Unfortunately, the ^{13}C NMR efforts did not stimulate much work by others, possibly because a home-built spectrometer was used for these studies and most laboratories were unable to achieve a similar performance. Furthermore, the signal resolution was rather poor, and the perturbation of similar spectra by solvent signals is a general problem.

It occurred to us that a new NMR approach should be rewarding, after we had obtained well-resolved solid-state ^{1}H,

(10) Miller, J. S.; Epstein, A. J. *Angew. Chem., Int. Ed. Engl.* **1994**, *33*, 385−415.

(11) (a) Yamaguchi, K.; Fueno, T.; Nakasuji, K.; Murata, J. *Chem. Lett.* **1986**, 629−632. (b) Yamaguchi, K.; Okumura, M.; Maki, J.; Noro, T.; Namimoto, N.; Nakano, M.; Fueno, T.; Nakasuji, K. *Chem. Phys. Lett.* **1992**, *190*, 353−360.

(12) (a) Deumal, M.; Novoa, J. J.; Bearpark, M. J.; Celani, P.; Olivucci, M.; Robb, M. A. *J. Phys. Chem. A* **1998**, *102*, 8402−8412. (b) Novoa, J. J.; Deumal, M.; Lafuente, P.; Robb, M. A.; *Mol. Cryst. Liq. Cryst.* in press.

(13) (a) Kreilick, R. W.; Becher, J.; Ullman, E. F. *J. Am. Chem. Soc.* **1969**, *91*, 5121−5124. (b) D'Anna, J. A.; Wharton, J. H. *J. Chem. Phys.* **1970**, *53*, 4047−4052. (c) Ullman, E. F.; Osiecki, J. H.; Boocock, D. G. B.; Darcy, R. *J. Chem. Phys.* **1972**, *94*, 7049−7059.

(14) (a) Cirujeda, J.; Hernàndez-Gasió, E.; Lanfranc de Panthou, F.; Laugier, J.; Mas, M.; Motins, E.; Rovira, C.; Novoa, J. J.; Rey, P.; Veciana, J. *J. Mol. Cryst. Liq. Cryst.* **1995**, *271*, 1−12. (b) Cirujeda, J., Thesis, Universitat Ramon Lull, Barcelona, 1997.

(15) (a) Ottaviani, M. F. *J. Chem. Soc., Faraday Trans.* **1990**, *86*, 3211−3219. (b) Takui, T.; Miura, Y.; Inui, K.; Teki, Y.; Inoue, M.; Itoh, K. *Mol. Cryst. Liq. Cryst.* **1995**, *271*, 55−66.

(16) (a) Zheludev, A.; Barone, V.; Bonnet, M.; Delley, B.; Grand, A.; Ressouche, E.; Rey, P.; Subra, R.; Schweizer, J. *J. Am. Chem. Soc.* **1994**, *116*, 2019−2027. (b) Zheludev, A.; Bonnet, M.; Ressouche, E.; Schweizer, J.; Wan, M.; Wan, H. *J. Magn. Magn. Mater.* **1994**, *135*, 147−160. (c) Pontillon, Y.; Ressouche, E.; Romero, F.; Schweizer, J.; Ziessel, R. *Physica B* **1997**, *234−236*, 788−789.

(17) (a) Davis, M. S.; Morokuma, K.; Kreilick, R. W. *J. Am. Chem. Soc.* **1972**, *94*, 5588−5592. (b) Neely, J. W.; Hatch, G. F.; Kreilick, R. W. *J. Am. Chem. Soc.* **1974**, *96*, 652−656. (c) Goldman, J.; Petersen, T. E.; Torssell, K.; Becher, J. *Tetrahedron* **1973**, *29,* 3833−3843.

Chart 1

^{2}H, and ^{13}C NMR spectra of paramagnetic metallocenes.[18] Only few NMR studies of solid organic radicals have been reported[19] before this work was started.[20] It was hoped that the spin distribution of nitronylnitroxides could be determined in pure crystalline samples so that the results were most closely related to the solid-state magnetic properties. Here we describe the magic angle spinning (MAS) ^{1}H,^{2}H, and ^{13}C NMR spectra of selected nitronylnitroxides **2**−**6** (Chart 1) with emphasis on the *o*-, *m*-, and *p*-hydroxyphenyl derivatives, the conversion of the NMR data to spin density maps, and the comparison with data obtained from ab initio calculations.

Results

^{13}C NMR Spectra. Figure 1a shows the ^{13}C MAS NMR spectrum of **6** as a typical example. The broad feature (B) at 111 ppm was shown to be a background signal from the probehead by running a spectrum with an empty rotor. Attempts to remove this feature by applying special pulse sequences[21] considerably decreased the signal-to-noise ratio of most other signals, and those shifted more than 1000 ppm disappeared. The probehead signal did not show up in the spectra of diamagnetic samples when the signals were enhanced by cross polarization (CP). However, CP did not work in the present experiments because of fast (T_2 < 1 ms) proton relaxation. Spinning sidebands were identified by running the spectrum at various MAS rates. The sharp signal (X) near 30 ppm belongs to a diamagnetic impurity. This became evident after changing the temperature, whereupon all signals moved as expected except for that near 30 ppm.

There are thus seven ^{13}C NMR signals remaining for **6,** which is one short if all carbon atoms are nonequivalent. The missing signal belongs to C2 which cannot be observed, because it carries too much spin. Theory predicts (see Discussion) that in the nitronylnitroxide moiety the spin densities at C4/5 and at the methyl carbons Cα4/5 should have different signs and that

(18) (a) Blümel, J.; Herker, M.; Hiller, W.; Köhler, F. H. *Organometallics* **1996**, *15*, 3474−3476. (b) Köhler, F. H.; Xie, X. *Magn. Reson. Chem.* **1997**, *35*, 487−492.

(19) (a) Ferrieu, F.; Nechstein, M.; *Chem. Phys. Lett.* **1971**, *11*, 46−50. (b) Ondercin, D.; Sandreczki, T.; Kreilick, R. W.; *J. Magn. Reson.* **1979**, *34*, 151−159. (c) Hentsch, F.; Helmle, M.; Köngeter, D.; Mehring, M.; *Ber. Bunsen-Ges. Phys. Chem.* **1987**, *91*, 911−913. (d) Groombridge, C. J.; Perkins, M. J. *J. Chem. Soc., Chem. Commun.* **1991**, 1164−1166. (e) Barrie, P. J.; Groombridge, C. J.; Grossel, M. C.; Weston, S. C.; *J. Chem. Soc.*, *Chem. Commun.* **1992**, 1216−1218. (f) Chen, J.; Cai, F.-F.; Shao, Q.-F.; Huang, Z.-E.; Chen, S.-M. *J. Chem. Soc., Chem. Commun.* **1996**, 1111−1112.

(20) Heise, H., Diploma Thesis, Technische Univeristät München, 1996.

(21) Corey, D. G.; Ritchey, W. M. *J. Magn. Reson.* **1988**, *80*, 128−132.
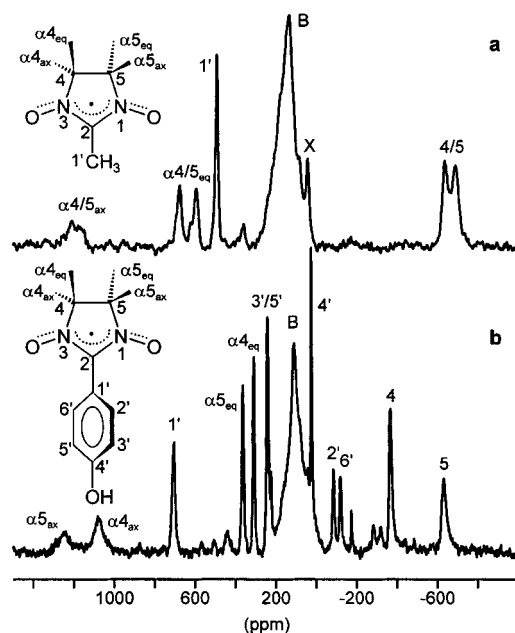
Figure 1. ^{13}C MAS NMR spectra of **6** (temperature: 303 K, spinning rate: 10 kHz) (a) and of **4** (temperature: 314 K, spinning rate: 15 kHz) (b). B is the background signal of the probehead, X is a diamagnetic impurity. Nonassigned signals are spinning sidebands.

Table 1. ^{13}C MAS NMR Data[a] of the Nitronylnitroxides **2**, **3**, **4**, **5**, and **6**

nucleus and position[b]	2	3	4	5[c]	6[d]
Cα4$_{ax}$	1180[e]	1075	1080	1060	1135
	1222[e]	**1111**	**1116**	**1095**	**1163**
Cα5$_{ax}$	705	1030	1250	1145	1170
	721	**1064**	**1295**	**1186**	**1199**
Cα4$_{eq}$	402	568	309	332	573
	402	**577**	**304**	**328**	**577**
Cα5$_{eq}$	360	568	363	418	650
	358	**577**	**361**	**419**	**657**
C4	−750	−707	−367	−470	−635
	−860	**−815**	**−457**	**−565**	**−732**
C5	−309	−617	−633	−590	−670
	−395	**−720**	**−737**	**−692**	**−768**
C1′	*f*	700	704	727	466
		592	**606**	**629**	**454**
C2′	−225	−118	−85	−120	
	−407	**−245**	**−229**	**−265**	
C3′	238	320	241	257	
	127	**172**	**132**	**150**	
C4′	52	−10.3	25	−4	
	−89	**−140**	**−146**	**−178**	
C5′	198	279	241	268	
	82	**157**	**132**	**162**	
C6′	−191	−178	−120	−139	
	−342	**−318**	**−265**	**−285**	

[a] Normal figures for experimental shifts at 314 K except for **6** with 311 K. Bold data for contact shifts at 298 K. [b] For numbering see Figures 1−5 and 7. [c] For OCH$_3$ the corresponding shifts are 179 and **130** ppm. [d] Signal interchange of the nuclei in positions 4/5 and α4/5 cannot be excluded. [e] Tentative, see next. [f] Not detected.
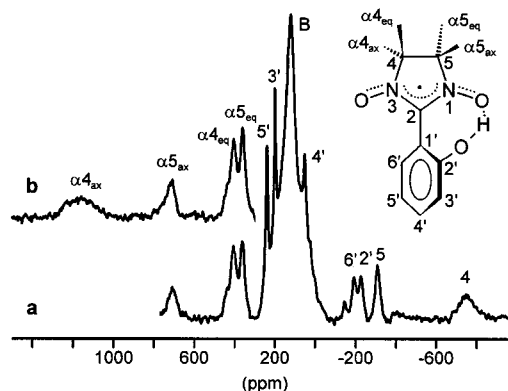

Figure 2. ^{13}C MAS NMR spectrum of **2** (temperature: 314 K, spinning rate: 15 kHz). B is the background signal of the probehead. (a) and (b) are the spectra optimized for low- and high-frequency signals, respectively. Nonassigned signals are spinning sidebands.

positive and negative spin gives rise to positive and negative signal shifts, respectively. Therefore, the two signals at low frequency must belong to C4/5, and the spin at C4/5 must be negative. At high frequency there are two pairs of signals which are assigned to Cα4/5; they are further distinguished (e.g., as axial and equatorial methyl groups) by arguments given in the Discussion. The remaining signal near 480 ppm which is remarkably narrow must belong to the CH$_3$ group labeled C1′.

The signal assignment of the ^{13}C MAS NMR spectrum of **4** (Figure 1b) follows from the comparison with that of **6** and with theory. In the crystal the molecular symmetry of **4** is C$_1$.[22a] There are two different molecules in the unit cell which are so similar that they could not be distinguished by NMR spectroscopy. On this basis 13 signals were expected of which 11 were found. Again C2 could not be observed, while the signals of C3′ and C5′ coincide. The latter followed from the intensity of the signal near 240 ppm; note that (little) separated signals were found for C3′ and C5′ of the radicals **2** and **5**. For the nitronylnitroxide moiety the signals of C4/5 and two of the four signals of Cα4/5 were identified by their shift signs and large shifts. Among the signals remaining at high-frequency those near 310 and 360 ppm were assigned to the second pair of Cα4/5, because very similar shifts were observed for the methoxy derivative **5** (Table 1). Both signal pairs of Cα4/5 of **5** could be identified in turn by their coalescence behavior at elevated temperature (see below).

There are five signals left for the hydroxyphenyl substituent of **4**. When spin polarization is the dominating delocalization mechanism[17] (see Discussion) the spin should be positive at C1′and C3′/5′ and negative at C2′/6′ and C4′. This was confirmed by the fact that the corresponding signals appeared at high and low frequency. C1′ gave a rather narrow, strongly

shifted signal similar to that of **6** (and the other compounds in Table 1) and in agreement with the calculations given below. Theory also predicts that the signal shifts should be similar for C2′/6′ and C3′/5′, respectively. Indeed, the spectrum shows that C3′/5′ are accidentally equivalent and that the signals of C2′/6′ are only 35.2 ppm apart; their distinction follows from the calculated spin densities. The signal which is left near 25 ppm belongs to C4′; note that after referencing its paramagnetic shift is negative as expected.

The spectrum of **3** and the remaining signals of **5** were assigned analogously; the data are collected in Table 1. The pattern of the ^{13}C MAS NMR spectrum of **2** (Figure 2) differs from that of **4** in a few details. While the signals of C2′−C6′ and Cα4/5$_{eq}$ were found in the known ranges, the narrow signal between 450 and 750 ppm that is characteristic of C1′ was missing. Rather, a signal appeared near 700 ppm of which the

(22) (a) Cirujeda, J.; Mas, M.; Molins, E.; Lanfranc de Panthou, F.; Laugier, J.; Park, J. G.; Paulsen, C.; Rey, P.; Rovira, C.; Veciana, J. *J. Chem. Soc., Chem. Commun.* **1995**, 709−710. (b) Hernàndez, E.; Mas, M.; Molins, E.; Rovira, C.; Veciana, J. *Angew. Chem., Int. Ed. Engl.* **1993**, *32*, 882−884.
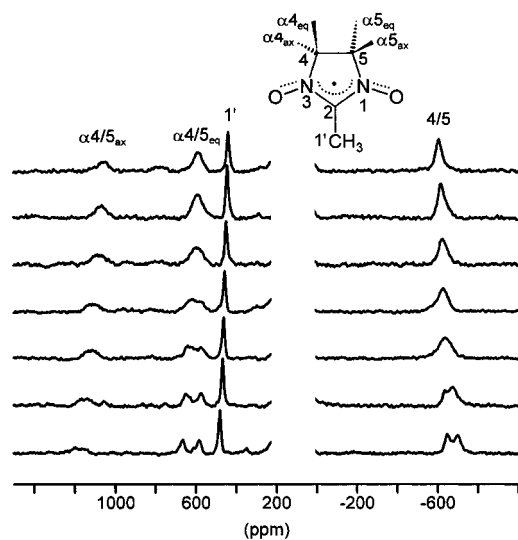
Figure 3. Variable-temperature ^{13}C MAS NMR spectra of **6** (spinning rate: 12 kHz). The temperatures from top to bottom are 331, 326, 322, 318, 314, 311, and 306 K, respectively. The signals of the background and an impurity have been omitted.

Figure 4. ^{1}H NMR spectra of (a) **4**, (b) **3**, and (c) **2** dissolved in acetone-d_6 at 305 K. (d) ^{2}H NMR of spectrum of **2**-d_1 dissolved in acetone at 305 K. S = solvent, X = diamagnetic impurities.

width is similar to those of the methyl groups Cα4/5$_{ax}$ (see Figure 1). At about 1180 ppm, where the signals of the axial methyl groups of **3**−**6** were found, only one broad and weak signal could be detected when the carrier frequency was close to resonance. Therefore, this feature is tentatively considered as the signal of one of the axial methyl groups. According to the calculated data given below it is assigned to Cα4$_{ax}$, while Cα5$_{ax}$ is left for the signal near 700 ppm. A correspondingly large signal separation was found for C4 and C5. Again the detection of the broad signal near −750 ppm was improved by optimizing the carrier frequency. As for C1′ we assume that its signal is covered by those of Cα4/5$_{eq}$ or Cα5$_{ax}$; in this context it should be noted that the high-frequency shoulder of the signal of Cα4$_{eq}$ in Figure 2 is a spinning sideband.

As can be seen in Table 1 the magnitude of the signal shift of C4/5 is typically smaller than 750 ppm. This is at variance with the interpretation of the ESR spectrum of *o*-tolylnitronyl-nitroxide.[13b] For C4/5 a ^{13}C hyperfine coupling constant of 6 G has been reported which would be equivalent to (−)1780 ppm.

The nitronylnitroxides **2**−**6** were also studied by temperature-dependent ^{13}C MAS NMR spectroscopy between 306 K and the temperature of slow decomposition (∼360 K), which was evident from the appearance of new signals in the shift range characteristic of diamagnetic compounds. A representative series of spectra is shown for **6** in Figure 3. It can be seen that the amount of the paramagnetic signal shift decreases when the temperature is raised as is expected from eq 1 in the Discussion. A similar series was recorded for **2**, but the temperature effect did not allow the coinciding signals mentioned above (C1′, Cα5$_{ax}$, Cα4/5$_{eq}$) to be separated. The most striking feature of Figure 3 is that the signal pairs of Cα4/5$_{ax}$, Cα4/5$_{eq}$, and C4/5 undergo coalescence at about 311, 314, and 320 K, respectively. Coalescence was also observed for **5** (345 K for Cα4/5$_{eq}$ and C4/5), while the number of signals did not change with temperature in the case of **2**−**4**.

^{1}H and ^{2}H NMR Spectra. Solutions of the three isomeric hydroxyphenylnitronylnitroxides **2**, **3**, and **4** gave the spectra reproduced in Figure 4. The basic signal assignment is straightforward and follows from the relative areas and the spin delocalization pattern which was confirmed by the ^{13}C NMR studies of the previous section. On passing from a given phenyl
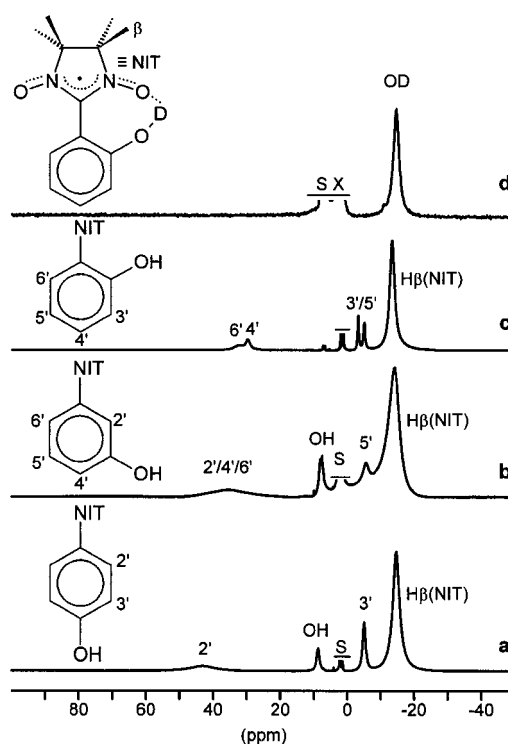
carbon atom to the neighboring proton further polarization inverts the spin sign, and positive spin is induced at H2′/6′ and H4′, while it is negative at H3′/5′. In fact, the corresponding signals appeared at high and low frequency, respectively. As distinct from solid-state structures, the structures we are dealing with here are averaged structures, which is indicated by a single signal for the methyl protons. In the case of **3** the signals of H2′/6′ and H4′ could not be resolved. H4′ and H6′ of **2** were distinguished by their signal widths, which are rather different while the shifts are similar. This means that the spin densities at the corresponding protons are very similar and that, therefore, contact relaxation[23] caused by the unpaired electron cannot be responsible for the different signal widths. Rather dipolar relaxation dominates, i.e., the relaxation rate increases with r^{-6} (r is the distance between the nucleus and the spin source located at the NO groups). It follows that the broader signal must belong to H2′/6′ which are closer to the NO groups than H4′. This agrees with our theoretical results and suggests to assign also the signals of H3′ and H5′ following the theory.

The remaining signal near 9 ppm in the spectra of **3** and **4** must be assigned to the hydroxy proton. Its shift decreased strongly with increasing concentration. By contrast, the OH signal could not be detected for **2**. When **2** was deuterated selectively the ^{2}H NMR spectrum showed an OD signal near 14 ppm (Figure 4d). Comparison with the ^{1}H NMR spectrum (Figure 4c) demonstrates that the OH signal is buried under the CH$_3$ signal.

The solid-state ^{1}H MAS NMR spectrum of **2** is reproduced in Figure 5 as a representative example of the nitronylnitroxides of this study. While a feature for H4′ and H6′ was clearly visible, the signals of the other protons were strongly overlapping so

(23) Kowalevski, J.; Nordenskiöld, L.; Benetis, N.; Westlund, P. O. *Prog. Nucl. Magn. Reson. Spectrosc.* **1985**, *17*, 141−185. Bertini, J. Luchinat, C. *NMR of Paramagnetic Molecules in Biological Systems;* The Benjamin/ Cumming Publishing Company: Menlo Park, 1986; Chapter 3.
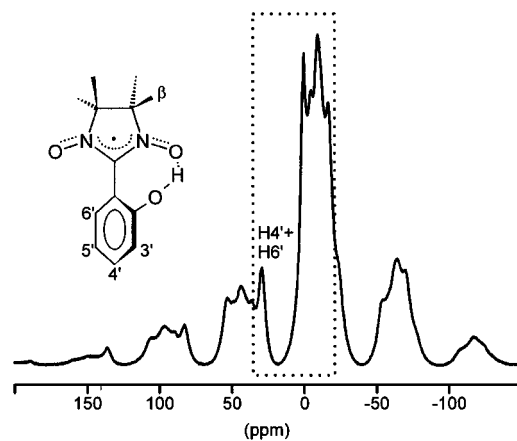
Spin Densities Determined by Solid-State NMR

J. Am. Chem. Soc., Vol. 121, No. 41, 1999 9663

Figure 5. ^{1}H MAS NMR spectrum of **2** (temperature: 315 K, spinning rate: 16 kHz). The centerbands are marked by the frame.
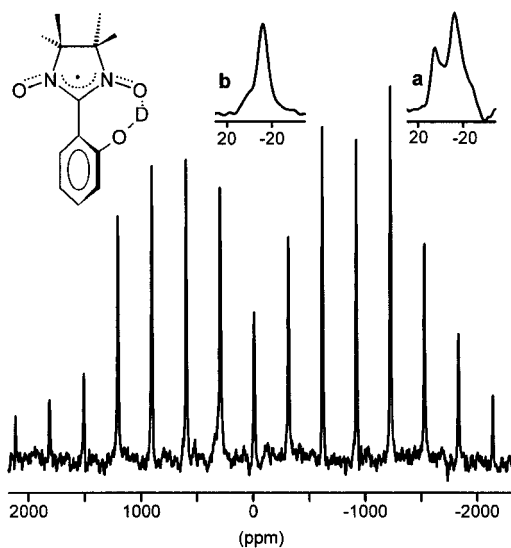

Figure 6. ^{2}H MAS NMR spectrum of **2**-d_1 (temperature: 311 K, spinning rate: 14 kHz). Insets (a) and (b): Expansions before and after removal of EtOD, respectively.

that they could not be assigned. In particular, the OH signal could not be localized. Therefore, the OD derivatives of **2, 3,** and **4** were investigated by ^{2}H MAS NMR spectroscopy. The spectra consisted of sideband patterns that had envelopes typical of spin-1 nuclei;[24] an example is given in Figure 6. Traces of EtOD from the deuteration procedure may be detected (inset a) in the sample. Its signal is useful as an internal reference in addition to external CDCl$_3$. Recrystallization from CH$_2$Cl$_2$ gave pure **2**-d_1 as can be seen from the overview spectrum of Figure 6 and inset b. Similar results were obtained for **3** and **4** (Table 2). The ^{1}H hyperfine coupling constants calculated from the NMR data deviate from those determined by the simulation of ESR spectra[14] by less than 8% except for H2′/H6′ of **3**. It is worth noting that ^{2}H NMR spectroscopy is the only method that yields information on the hydroxy groups which are crucial for intermolecular spin interaction.

The ^{1}H MAS NMR spectrum of **6** in Figure 7 shows an unusually shifted signal at −230.6 ppm and a feature near −13 ppm. The latter is characteristic of methyl groups bound to C4 and C5 and consists of two overlapping signals, a broad and a narrow one. The broad signal was assigned to the axial methyl

(24) Ackerman, J. L.; Eckman, R.; Pines, A. *Chem. Phys.* **1979**, *42*, 423−428.

Table 2. Solution- and Solid-State ^{1}H and ^{2}H NMR Data[a] of the Nitronylnitroxides **2**, **3**, **4**, **5**, and **6**

nucleus and position[b]	2	3	4	5[c]	6[d]
Hβ4/5, solution	−13.2	−14.2	−14.7	−14.6	
	−14.6	**−15.6**	**−16.2**	**−16.0**	
Hβ4/5$_{ax}$, solid					−13.1
					−14.8
Hβ4/5$_{eq}$, solid					−13.9
					−15.6
H1′, solid					−230.6
					−243.0
Hα2′/6′, solution	32.4	35.6	43.1	42.0	
	25.5	**28.9**	**36.1**	**35.1**	
Hα2′/6′, solid	29.3	43.0	34.6		
	23.0	**37.6**	**28.3**		
Hα3′, soluton	−3.2[g]			−5.1	−5.2
	−10.3		**−12.4**	**−12.7**	
Hα4′, solution	29.9	35.6			
	23.0	**29.1**			
Hα4′, solid	29.3	40.0[e]			
	23.0	**34.6**			
Hα5′, solution	−5.0[g]	−5.6	−5.1	−5.2	
	−12.2	**−13.3**	**−12.4**	**−12.7**	
OH, solution		7.9	8.6		
		−2.1	**−2.0**		
OD solution	−14.4				
	−25.9				
OD, solid[f]	−12.1	11.8	0.2		
	−24.0	**1.9**	**−10.9**		

[a] Bold data for contact shifts at 298 K. Normal figures for experimental shifts; solution spectra (acetone-d_6) at 305 K, solid-state spectra at 314 K, unless stated otherwise. [b] For numbering see Figures 1−5 and 7. [c] For OCH$_3$ the corresponding shifts are 0.3 and **−2.1** ppm. [d−f] Experimental shifts at 312, 304, and 311 K, respectively. [g] Distinction of Hα3′/5′ based on calculated spin densities.
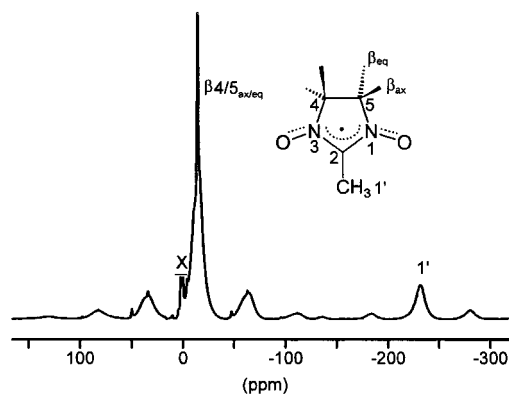

Figure 7. ^{1}H MAS NMR spectrum of **6** (temperature: 314 K, spinning rate: 14.5 kHz). Nonassigned signals are spinning sidebands, X = diamagnetic impurity.

groups, because they are closer to the spin source NO, thus making dipolar relaxation more efficient. Signal deconvolution gave the data listed in Table 2. Obviously, the remaining strongly shifted signal must belong to the methyl group bound to C2 (H1′).

Discussion

Conversion of the NMR Data to Spin Densities. The experimental NMR signal shifts, δ^{exp}, of paramagnetic species are composed of a paramagnetic contribution, δ^{para}, and a diamagnetic contribution, δ^{dia}. Here we are interested in the effect of the unpaired electron on the NMR signal shifts of the nitronylnitroxide radicals. This effect is described by the hyperfine coupling constant $A(n)$ between the electron and the nuclear spins. $A(n)$ is related to the contact shift, δ^{con}, by eq 1
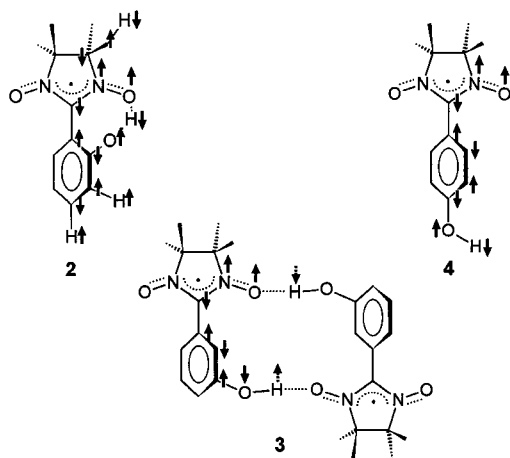
Figure 8. Experimental sign patterns of the spin densities for **2**, **3**, and **4**. Up-spins indicate positive spin. Dotted arrows result from formally continuing the respective polarization path.

and to the unpaired electron spin density, ρ_n, at any observed nucleus n by eq 2:[25]

$$A(n) = \frac{4\gamma_n kT}{g_e \beta_e} \delta^{con} \tag{1}$$

$$A(n) = \frac{2}{3} \mu_0 g_e \beta_e \gamma_n \rho_n \tag{2}$$

In eqs 1 and 2 γ_n is the gyromagnetic ratio, k is the Boltzmann factor, T is the absolute temperature, g_e is the electron g factor, β_e is the Bohr magneton, and μ_0 is the vacuum permeability.

In the present cases $\delta^{con} = \delta^{para}$ is a good approximation, because the dipolar shift contributions, δ^{dip},[25] to δ^{para} are negligible owing to the generally small g-factor anisotropy.[13b] Since δ^{con} is proportional to $1/T$ (eq 1), it can be obtained by recording temperature-dependent spectra. In a δ^{exp}-versus-T^{-1} diagram the intercept is δ^{dia}, and the desired contact shift is $\delta^{con} = \delta^{exp} - \delta^{dia}$. However, the data analysis resulted in considerable errors for the broad signals. Therefore, the signal shifts of most similar diamagnetic compounds were taken as δ^{dia}-values (Supporting Information) and subtracted from the respective δ^{exp}-values in order to obtain the δ^{con}-values. Owing to different rotor spinning rates the spectra could not be recorded at the same temperature. To ensure a reliable comparison of the data all δ^{con}-values were calculated for the standard temperature 298 K (bold data in Tables 1 and 2). This is based on the fact that that the molar susceptibility χ_m of the radicals in question varies linearly with T^{-1} above 100 K[7] and that χ_m is proportional to δ^{para}.[25] Conversion of the δ^{con} values to the spin densities by using eqs 1 and 2 and a mean g-factor of 2.006[13,26] gave the data in Table 3.

Intramolecular Electron Delocalization. As can be seen from eqs 1 and 2, the sign of the NMR signal shift and the spin density is the same. When these signs (Tables 1−3) are visualized as arrows, the patterns shown in Figure 8 are obtained. They are characteristic of spin polarization and confirm previous conclusions derived from magnetic resonance[15,17] and PND.[16]

Another characteristic feature are the pairwise very different NMR signal shifts of the four methyl carbon atoms of **3**−**6**

(25) (a) La Mar, G. N.; Horrocks, W.; DeW., Jr., Holm, R. H., Eds. *NMR of Paramagnetic Molecules*; Academic Press: New York, 1973, (b) Drago, R. S. *Physical Methods for Chemists*; Saunders College Publishing: Ft. Worth, 1992, Chapter 12.
(26) Cirujeda, J.; Hernàndez-Gasió, E.; Rovira, C.; Stanger, J. L.; Turek, P.; Veciana, J. *J. Mater. Chem.* **1995**, *5*, 243−252.
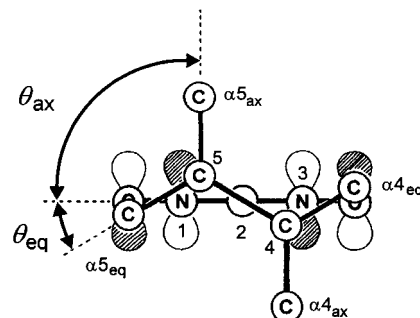

Figure 9. Side view of an unsubstituted nitronylnitroxide down from the center of the bond C4−C5 to C2. The spin-carrying MO is located on the NO groups.
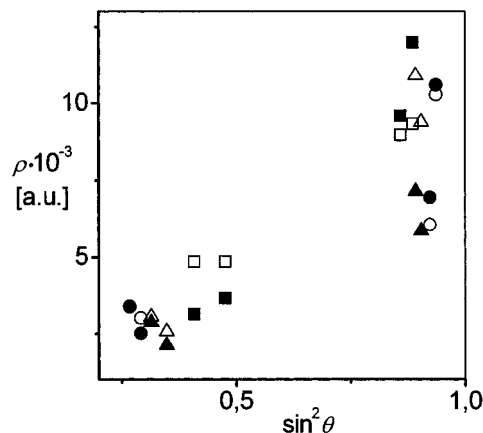

Figure 10. Dependence of experimental (open symbols) and the calculated spin densities (filled symbols) of Cα of **2** ($\bigcirc,\bullet$), **3** ($\square,\blacksquare$), and **4** ($\triangle,\blacktriangle$) on the dihedral angle θ (see text).

(Figure 1 and Table 1). This is indicative of axial and equatorial methyl groups which result from puckering of the imidazolyl moiety in keeping with crystal structure results.[22] As can be seen in Figure 9, there is efficient hyperconjugational interaction between the spin-carrying MO at nitrogen with the axial bond C5−Cα5$_{ax}$ while for the corresponding equatorial bond it is less efficient. Thus, more spin is transmitted to Cα5$_{ax}$ than to Cα5$_{eq}$, and this is reflected in the NMR signal shifts. When the crystal data are considered, a convenient approach is to relate δ^{con} with, for instance, the angle θ between the bond C5−Cα5$_{ax}$ (or C5− Cα5$_{eq}$) and the plane containing O1, N1, C2, and C5:

$$\delta^{con}(C\alpha 5_{ax}) = \delta_o(C\alpha 5_{ax}) + B \sin^2 \theta_{ax} \tag{3}$$

Equation 3 has been adapted from early ESR work.[27] Its second term reflects hyperconjugation with B being a constant, while the first term is the sum of all other shift contributions. The same reasoning applies for Cα4$_{ax/eq}$.

The imidazole puckering in Figure 9 is idealized. In the crystal the angles θ are slightly different for the two axial and equatorial methyl groups, respectively. This is why pairs of signals were observed for both Cα4/5$_{ax}$ and Cα4/5$_{eq}$. Another consequence of the low symmetry is that in eq 3 B is no longer a constant. Rather B(N1) and B(N2) must be distinguished, because the spin density at N1 and N2 is different, and δ_o must vary as well. This is confirmed by a plot of the experimental spin densities (calculated from δ^{con}, Table 3) over $\sin^2 \theta$ (Figure 10). As expected, Cα4/5$_{ax}$ and Cα4/5$_{eq}$ are found in well-separated ranges. However, there is considerable scatter in each range, which means that the straight lines passing through pairs such

(27) Heller, C.; McConnell, H. M. *J. Chem. Phys.* **1960**, *32*, 1535−1539.

Table 3. Calculated[a] and Experimental Spin Densities[b] of the Solid Nitronylnitroxides **2**, **3**, and **4**

nucleus and position[c]	2		3		4	
	ρ^{calcd}	ρ^{exp}	ρ^{calcd}	ρ^{exp}	ρ^{calcd}	ρ^{exp}
$C\alpha4_{ax}$	10.59	10.3[f]	12.00	9.3	5.83	9.4
$C\alpha5_{ax}$	6.95	6.1	9.58	8.9	7.14	10.9
$C\alpha4_{eq}$	3.39	3.38	3.15	4.85	2.11	2.56
$C\alpha5_{eq}$	2.51	3.01	3.67	4.85	2.87	3.04
C2	−33.93	g	−42.82	g	−42.68	g
C4	−7.65	−7.23	−8.01	−6.85	−5.90	−3.84
C5	−3.86	−3.32	−7.54	−6.05	−7.06	−6.20
C1′	8.16	g	12.11	4.98	12.43	5.10
C2′	−5.55	−3.42	−7.02	−2.06	−7.69	−1.92
C3′	1.89	1.07	5.30	1.45	4.35	1.11
C4′	−2.83	−0.75	−6.42	−1.17	−5.48	−1.22
C5′	2.18	0.69	5.04	1.32	4.44	1.11
C6′	−4.94	−2.88	−7.78	−2.67	−8.00	−2.23
Hβ4/5[d]	−0.06[h]	−0.12	−0.09[h]	−0.13	−0.10[h]	−0.14
Hα2′/6′	0.36	0.19	0.73[e]	0.32	0.64[e]	0.23
Hα3′[d]	−0.18	−0.09			−0.40	−0.10
Hα4′	0.31	0.19	0.70	0.29		
Hα5′[d]	−0.20	−0.10	−0.40	−0.11	−0.37	−0.10
OH/OD	−0.62	−0.20	−0.04	0.02	0.15	−0.09
N1	58.96	g	63.13	g	69.74	g
N3	64.06	g	65.27	g	59.11	g
O1	48.08	g	79.96	g	84.02	g
O3	95.83	g	76.95	g	72.16	g

[a] B3LYP functionals, cc-pVDZ double-ζ quality basis set. [b] In atomic units $\times 10^{-3}$. [c] For numbering of the nuclei see Figures 1−5 and 7. [d] Experimental data available only for solution. [e] Mean value of Hα2′ and 6′. [f] Tentative, see text. [g] Not detected. [h] Averaged value of rotating CH₃.

as $C\alpha4_{ax}$ and $C\alpha4_{eq}$ have different intercepts and slopes, or, according to eq 3, different δ_o and B values.

First-order hyperconjugation selectively transmits spin to nuclei separated from the source by two bonds. Therefore, H1′ and Cα of **6** are affected in the same way. The selective spin transfer to H1′ is reflected in a large contact shift of −243.7 ppm. Conversion of this shift to the hyperfine coupling constant by (a reformulated version of) eq 2 yields 3.27 G which is in good agreement with ESR results.[13c]

Comparison of Experimental and Theoretical Results. The spin densities at the various nuclei of **2**, **3**, and **4** were calculated by ab initio methods, and the resulting data are compared to the experimental spin densities in Table 3. The agreement is reasonable, but the experimental spin densities are generally smaller and seem to indicate a less pronounced polarization effect. The spin densities calculated previously by ab initio methods[16a,28] are similar to those reported here. Thus we find that the unrestricted Hartree−Fock method overestimates the polarization due to the large spin contamination of the ground state by states of higher multiplicity, a fact also found when semiempirical approaches to the Hartree−Fock method, like the INDO method are employed.[29] This overestimation effect is corrected when DFT functionals are employed which reproduce the experimental spin densities very well, although they slightly underestimate the polarization effect. Our experimental spin densities at the carbon atoms of **2−6** are in rough agreement with those obtained by PND for phenylnitronylnitroxide.[16a] PND gave a larger difference of the spin at the axial and equatorial methyl groups, the average amount of spin at the phenyl carbons

was about eight times larger, and, most strikingly, the spin at C5 was positive, while it is negative for all nitronylnitroxides of this study as expected from theory. The differences of NMR and PND results may be partly ascribed to the fact that both methods probe the spin densities differently. While NMR spectroscopy monitors the effect that the spin density has on the nuclei, PND observes the spin populations represented by atomic and molecular orbitals.

The shift of the missing ¹³C NMR signal of C2 can be estimated from the calculated spin to appear between −4000 and −5000 ppm. Also, a unique hyperfine coupling constant of 12 G has been reported for C2 of *o*-tolylnitronylnitroxide[13b] which is equivalent to about −3550 ppm. We were unable to detect C2 in the range up to −4500 ppm most probably because the width of the isotropic signal and the chemical shift anisotropy are too large.

The selective spin transfer by hyperconjugation from N1 and N2 to $C\alpha5_{ax}$ and $C\alpha4_{ax}$, respectively, which is evident from the NMR data (Figure 10) is also reflected by the calculated spin densities (Table 3). The latter data for $C\alpha4/5$ of **2**, **3**, and **4** plotted over $\sin^2\theta$ are combined with the NMR results in Figure 10. It can be seen that the scatter of the theoretical and experimental data for the axial and equatorial methyl groups is similar. Hence, the assignment of the corresponding NMR signals is tentative in as far as it follows slightly different calculated spin densities.

Effects of Hydrogen Bridging. Besides detailed spin density maps of **2−6** a principal goal was to get new insight in the hydrogen bridging between the nitronylnitroxides, because they have been proposed to be responsible for magnetic ordering.[7a,26,30] In careful parallel work on tetramethylpiperidinyloxyl radicals[31a] and pyridylnitronylnitroxide[31b] the usefulness of the ¹H and ²H NMR approach has been demonstrated. We have used deuteriation for both selective labeling and resolution enhancement, which is different in solution[32a] and in the solid state.[32b]

Among the hydroxyphenylnitronylnitroxides **2**, **3**, and **4** the ortho derivative **2** is unique in featuring almost the same OD signal shift in solution and in the solid state (Table 2), whereas the corresponding shifts of **3** and **4** differ considerably. Also, in solution the HO signal shifts of **3** and **4** were found to decrease with increasing concentration. This is indicative of different types of hydrogen bridges. In solid **3** and **4** the OH signal shift is influenced by *inter*molecular OH⋯ON bridges which are much less efficient in solution. By contrast, in **2** the predominating OH⋯ON bridge is *intra*molecular so that it is hardly affected by solvents such as acetone. As for the solids these conclusions are in keeping with the crystal structures.[22]

Another striking consequence of the intramolecular OH⋯ON bridge are the large differences of the NMR signal shifts of C4 and C5 and of $C\alpha4_{ax}$ and $C\alpha5_{ax}$, respectively. They reflect an unusual imbalance of the spin density on the two NO groups, which is most pronounced for the corresponding oxygen atoms (Table 3). It follows that when a high spin concentration on only one of the NO groups is desired, the approach can be monitored by ¹³C NMR spectroscopy.

(28) (a) Grand, A.; Rey, P.; Subra, R.; Barone, V. Minichino, C. *J. Chem. Phys.* **1991**, *95*, 9283−9242. (b) Barone, V. Grand, A.; Luneau, D.; Rey, P.; Minichino, C.; Subra, R. *New J. Chem.* **1993**, *17*, 545−549. (c) Novoa, J. J.; Mota, F.; Veciana, J.; Cirujeda, J. *Mol. Cryst. Liq. Cryst.* **1995**, *271*, 79−90.

(29) Yamaguchi, K.; Okamura, M.; Nakano, M. *Chem. Phys. Lett.* **1992**, *191*, 237−244.

(30) (a) Veciana, J.; Cirujeda, J.; Rovira, C.; Molins, E.; Novoa, J. J. *J. Phys. I France*, **1996**, *6*, 1967−1986. (b) Matsushita, M. M.; Izuoka, A.; Sugawara, T.; Kobayashi, T.; Wada, N.; Takeda, N.; Ishikawa, M. *J. Am. Chem. Soc.* **1997**, *119*, 4369−4379. (c) Kawakami, T.; Takeda, S.; Mori W.; Yamaguchi, K. *Chem. Phys. Lett.* **1996**, *261*, 129−137. (d) Lang, A.; Pei, Y.; Ouahab, L.; Kahn, O. *Adv. Mater.* **1996**, *8*, 60−62.

(31) (a) Maruta, G.; Takeda, S.; Imachi, R.; Ishida, T.; Nogami, T.; Yamaguchi, K. *J. Am. Chem. Soc.* **1999**, *121*, 424−431. (b) Murata, G.; Takeda, S.; Yamaguchi, A.; Okuno, T.; Awaga, K.; Yamaguchi, K. *Mol. Cryst. Liq. Cryst.*, submitted.

(32) (a) Laukien, G.; Noack, F. *Z. Phys.* **1960**, *159*, 311−332. (b) Nayeem, A.; Yesinowski, J. P. *J. Chem. Phys.* **1988**, *89*, 4600−4608.

9666   *J. Am. Chem. Soc., Vol. 121, No. 41, 1999*

Heise et al.

The spin sign patterns given in Figure 8 illustrate that the polarization path via the phenyl C-atoms entails negative spin on the hydrogens 2′-O*H* and 4′-O*H* and positive spin on 3′-O*H*. The second path would involve the nuclei NO⋯*H*O and induce negative spin regardless whether the hydrogen bridge is intramolecular (**2**) or intermolecular (**3** and **4**). Indeed, in **3** both pathways are similarly efficient, and the opposite spin contributions almost cancel ($\rho(OD) = 0.02$). In **2** and **4** both contributions add, appreciable negative spin is accumulated at O*H* or O*D*, and **2** is more affected ($\rho(OD) = -0.20$) than **4** ($\rho(OD) = -0.09$). It is worth noting that these results could be reproduced reasonably well by the theoretical calculations for **2**, but less so for **3** and **4** (Table 3). This is not surprising, because intermolecular interactions were not included in the calculations.

The NMR results also establish the importance of hydrogen bridges to fixing the radicals in the crystal. This follows from the temperature-dependent experiments. The signal coalescence for C4/5, Cα4/5$_{ax}$, and Cα4/5$_{eq}$ of **5** and **6** (Figure 3) suggests that the imidazole moiety vibrates in such a way that the nonequivalent nuclei are averaged out. The barriers of the dynamic process ($\Delta G^{\ddagger}_{coal}$) at the coalescence temperature (T_{coal}) of the signals can be determined from the corresponding shifts at T_{coal}[33] which in turn is extrapolated from the temperature series. For **5** and **6** the barriers were $\Delta G^{\ddagger}(C\alpha4/5_{eq}) = 57$ kJ mol^{-1} at 345 K and $\Delta G^{\ddagger}(C\alpha4/5_{eq}) = 54$ kJ mol^{-1} at 320 K, respectively. Similar barriers were obtained from the coalescence of the signals of C4/5 while T_{coal} could not be determined precisely for Cα4/5$_{ax}$.

The barriers cannot be attributed to rapid rotation or oscillation of the substituents at C2, because the rotation of the methyl group at C2 of **6** is not hindered at room temperature and above, as can be seen from a single proton resonance near −230 ppm (Figure 7). Also, inversion of the conformation of the five-membered ring is not responsible. This process would average out all four αCH$_3$ signals; it is only observed in solution (Figure 4), where the intermolecular interactions are weak, but not in the crystal. The solid-state dynamics strikingly depend on the presence of OH⋯ON bridges: Without OH groups (radicals **5** and **6**) the barrier is low, with OH groups (radicals **2**, **3**, and **4**) it is too high to be observed before decomposition takes place.

Conclusions and Prospects

Solid-state ^{13}C MAS NMR spectroscopy allows the structure of nitronylnitroxide radicals to be determined in much the same way as is known for diamagnetic molecules. Thus, geometrical details such as special ring conformations and lattice-imposed lowering of the molecular symmetry can be studied. In addition to the local molecular structure lattice properties may be probed via solid-state dynamics; an example is the freezing of vibrations of the nitronylnitroxide core by introducing OH⋯ON bridges.

The spectra are also useful for checking samples before subjecting them to magnetic measurements. Diamagnetic and paramagnetic byproducts and decomposition products can be detected as shown in the case of 2-methylnitronylnitroxide **6**.

The resolution of the ^{1}H MAS NMR spectra of nitronylnitroxides is not as good as that of the ^{13}C MAS NMR spectra, but it can be improved by using deuteriated compounds and ^{2}H MAS NMR spectroscopy. In this way intra- and intermolecular OH⋯ON bridges can be distinguished.

Conversion of NMR signal shifts into spin densities yields rather complete spin maps. In particular the determination of

the spin sign is simple. From spin maps the spin delocalization mechanism may be deduced. Thus, for nitronylnitroxides hyperconjugation and spin polarization has been confirmed. A regular polarization scheme is maintained up to remote nuclei like the OH groups of the isomeric hydroxyphenylnitronylnitroxides **2**, **3**, and **4**. When more than one polarization path is available in a radical spin cancellation or amplification may be observed. The experimental spin densities are in agreement with ab initio calculations on isolated radicals; deviations occur when intermolecular interactions are important.

Solid-state NMR spectroscopy proves to be a method for spin mapping that can be an alternative to polarized neutron diffraction (PND). The results obtained by both methods differ, because the spin is observed in different spaces. Limitations of the NMR method are (i) Nuclei with high spin density cannot be detected (e.g., N, O, and C2 of nitronylnitroxides). (ii) Detailed signal assignment must be sometimes supported by theoretical calculations. (iii) Often deuteriation and ^{2}H NMR studies must be performed. Advantages are (i) NMR experiments are cheaper than PND. (ii) No single crystals are necessary. (iii) Temperature-dependent studies may be carried out which yield information on solid-state dynamics as in this work and magnetic interactions as shown previously for transition metal complexes.[34] (iv) Spin densities at protons (or deuterons) are much easier to obtain by NMR than by PND. (v) Small spin densities at carbon atoms can be determined rather accurately, because usually the corresponding NMR signals are narrow.

It is expected that the method is applicable to many simple radicals, exchange-coupled oligomeric radicals, and radicals that are coordinated to paramagnetic and diamagnetic transition metal centers. The resulting spin maps would help to understand the interactions in molecular magnets.

Experimental Section

Nitronylnitroxides **2**−**6** were prepared following the general procedure described by Ullman et al.[3,13c,14c] Selective exchange of phenolic hydrogens for deuterium to obtain **2**-d_1, **3**-d_1, and **4**-d_1 was effected by repeated recrystallization from EtOD. The products were freed from EtOD under vacuum, and traces were removed by recrystallization from methylenechloride. X-ray powder diffraction confirmed that **2**-d_1 was still the β-phase.

All NMR measurements were carried out with a Bruker MSL 300 spectrometer. ^{1}H solution NMR spectra were measured in the routine high-resolution setup, and ^{2}H solution NMR spectra were recorded in the high-power setup, using a solenoid probehead with sample tubes of 10 mm diameter. For MAS NMR spectra the microcrystalline nitronylnitroxides were mixed with 5−10 mg of nickelocene, and the powder was packed into ZrO$_2$ and Si$_3$N$_4$ rotors with a diameter of 4 mm and sealed with Kel-F and BN caps. The FIDs were sampled after applying single pulses (duration 4 μs), delays of 8−14 μs for detector recovery, and repetition times of 200−400 ms. Spectra were improved by reverse linear prediction, line broadening up to the matched filter, and baseline correction. The temperature was measured internally for each sample by observing the calibrated temperature-dependent proton signal shift of nickelocene; the error was ±1 K. When the observed nucleus was ^{2}H and ^{13}C, this was done via the decoupling channel during a running MAS experiment. The procedure was completely analogous to that described for the vanadocene thermometer.[18b] The ^{1}H NMR spectrum of **6** was measured with and without (Figure 7) addition of nickelocene, because the nickelocene signal appears close to that of H1′ of **6**. Signal shifts in solution and in the solid state were measured relative to the solvent (acetone-d_6, $\delta(^1H) = 2.04$) and external adamantane $\delta(^1H) = 2.0$, $\delta(^{13}CH_2) = 29.5$), respectively. A rotor filled with CDCl$_3$ was used as external reference ($\delta(^2H) = 7.2$). The diamagnetic reference shifts were taken from the dihydroprecursors of

(33) Sandström, J. *Dynamic NMR Spectroscopy*; Academic Press: London, 1982; Chapter 7.

(34) Oldfield, E.; Walter, T. H. *J. Chem. Soc., Chem. Commun.* **1987**, 646−647. Campbell, G. C.; Haw, J. F. *Inorg. Chem.* **1988**, *27*, 3706−3709.

the nitronylnitroxides and appropriate hydroxybenzaldehydes (Supporting Information).

Theoretical spin densities were calculated on the ab initio level by using the B3LYP density functional[35] implemented in GAUSSIAN-94[36] and the cc-pVDZ double-ζ quality basis set.[37] The B3LYP method is known to give results close to the experiment and to the QCISD(T) method for π radicals which do not contain nitrogen.[38] The geometries of the radicals were taken from crystal structure results,[22] and the hyperfine coupling constants were calculated by using eq 1.

(35) Becke, A. D. *J. Chem. Phys*. **1993**, *98*, 5648−5652. Yang, W. *Density functional theory of Atoms and Molecules*; Oxford University Press: New York, 1989.

(36) Frisch, M. J.; Trucks, G. W.; Schlegel, H. B.; Gill, P. M. W.; Johnson, B. G.; Robb, M. A.; Cheeseman, J. R.; Keith, T.; Peterson, G. A.; Montgomery, J. A.; Raghavachari, K.; Al-Laham, M. A.; Zakrzewski, V. G.; Ortitz, J. V.; Foresman, J. B.; Ciolowski, J.; Stefanov, B. B.; Nanayakkara, A.; Challakombe, M.; Peng, C. Y., Ayala, P. Y.; Chen, W.; Wong, M. W.; Andres, L. J.; Replogle, E. S.; Gomperts, R.; Martin, R. L.; Fox, D. J.; Binkley, J. S.; Defrees, D. J.; Baker, J.; Stewart, J. J. P.; Head-Gordon, M.; Gonzalez, C.; Pople, J. A. Gaussian 94, Revision C.3; Gaussian Inc.: Pittsburgh, PA, 1995.

(37) Woon, D. E.; Dunning, T. H. *J. Chem. Phys.* **1993**, *98*, 1358−1371.

Supporting Information Available: NMR signal shifts of diamagnetic reference compounds (PDF). This material is available free of charge via the Web at http://pubs.acs.org.

JA991188T

(38) (a) Adamo, C.; Barone, V.; Fortunelli, A. *J. Chem. Phys*. **1995**, *102*, 384−393. (b) Barone, V.; Bencini, A.; Di Matteo, A. *J. Am. Chem. Soc.* **1997**, *119*, 10831−10837.